Supplementary Materials for

Structural Connectivity Matures Along a Sensorimotor-association Connectional Axis in Youth

Xiaoyu Xu[1,2], Hang Yang[2], Jing Cong[1,2], Valerie Sydnor[3], Zaixu Cui[2*]

*Correspondence: cuizaixu@cibr.ac.cn

Supplemental information

Supplementary Text

Results of sensitivity analyses

We conducted several sensitivity analyses to evaluate the robustness of our findings to methodological variation. In our primary analyses, we parcellated the cortex into 12 large-scale systems. Here, we found that our main findings were stable when examining 7 or 17 cortical systems. Across both resolutions, we observed significant associations between the second derivatives and S-A connectional axis ranks across all connections in HCP-D (7 system: rho = 0.88, $P < 0.001$, **Figure S4A**; 17 system: rho = 0.77, $P < 0.001$, **Figure S5A**). The critical age of zero alignment between the S-A connectional axis and connectome-wide developmental pattern was approximately 15.5 years with 7 systems (**Figure S4B**) and 15.5 years with 17 systems (**Figure S5B**). Within ABCD dataset, we consistently observed that S-A connectional ranks were associated with both age effects (7 system: rho = -0.81, $P < 0.001$, **Figure S4C**; 17 system: rho = -0.61, $P < 0.001$, **Figure S5C**) and the second derivatives (7 system: rho = 0.88, $P < 0.001$, **Figure S4D**; 17 system: rho = 0.75, $P < 0.001$, **Figure S5D**) across all connections. Furthermore, the associations between structural connectivity strength and both higher-order cognition and general psychopathology factor were patterned on the connectome along the S-A connectional axis with both 7 systems (cognition: rho = -0.40, $P < 0.001$, **Figure S4E**; *p*-factor: rho = 0.60, $P < 0.001$, **Figure S4F**) and 17 systems (rho = -0.22, $P = 0.005$, **Figure S5E**; *p*-factor: rho = 0.33, $P < 0.001$, **Figure S5F**) cortical parcellation.

Second, we evaluated whether our results were stable after controlling for the Euclidean distance between pairwise systems when correlating the statistical maps and S-A connectional axis rank. We found all the results were similar to our primary findings. Specifically, the second derivatives of developmental trajectories still exhibited a strong correlation with the S-A connectional axis ranks (rho = 0.74, $P < 0.001$, **Figure S6A**) and the critical age of zero alignment between the S-A connectional axis and connectome-wide developmental effects was approximately 15.7 years (**Figure S6B**) in HCP-D. In the ABCD dataset, strong correlations between the S-A connectional axis and both the age effects (rho = -0.56, $P < 0.001$, **Figure S6C**) and the second derivatives (rho = 0.78, $P < 0.001$, **Figure S6D**) were observed. The cognitive associations with structural connectivity strength were marginally significantly related to the S-A connectional axis ranks (rho = -0.19, $P = 0.091$, **Figure S6E**), while the psychopathological associations with structural connectivity strength were significantly correlated to the S-A connectional axis ranks (rho = 0.45, $P < 0.001$, **Figure S6F**).

Third, we demonstrated that our statistical results remain stable after controlling for additional covariates, including social-economic status (SES) and intracranial volume (ICV). Particularly, after separately controlling for ICV or SES additionally, the second derivatives still exhibited a strong correlation with the S-A connectional axis ranks (SES control: rho = 0.80, $P < 0.001$, **Figure S7A**; ICV control: rho = 0.84, $P < 0.001$, **Figure S8A**) and the critical age of zero alignment between the S-A connectional axis and connectome-wide developmental effects was approximately 15.5 years (SES control: **Figure S7B**; ICV control: **Figure S8B**) in the HCP-D dataset. In the ABCD dataset, strong correlations between the S-A connectional axis and both the age effects (SES control: rho = -0.69, $P < 0.001$, **Figure S7C**; ICV control: rho = -0.66, $P < 0.001$, **Figure S8C**) and the second derivatives (SES control: rho = 0.82, $P < 0.001$, **Figure S7D**; ICV control: rho = 0.82, $P < 0.001$, **Figure S8D**) were observed. Furthermore, the associations between structural connectivity strength and both higher-order cognition and general psychopathology factor were patterned on the connectome along the S-A connectional axis while both additionally

controlling for SES (cognition: rho = -0.41, $P < 0.001$, **Figure S7E**; *p*-factor: rho = 0.48, $P < 0.001$, **Figure S7F**) and additionally controlling for ICV (cognition: rho = -0.22, $P = 0.051$, **Figure S8E**; *p*-factor: rho = 0.50, $P < 0.001$, **Figure S8F**).

Overall, these analyses demonstrated the robustness of our results to the methodological variations.

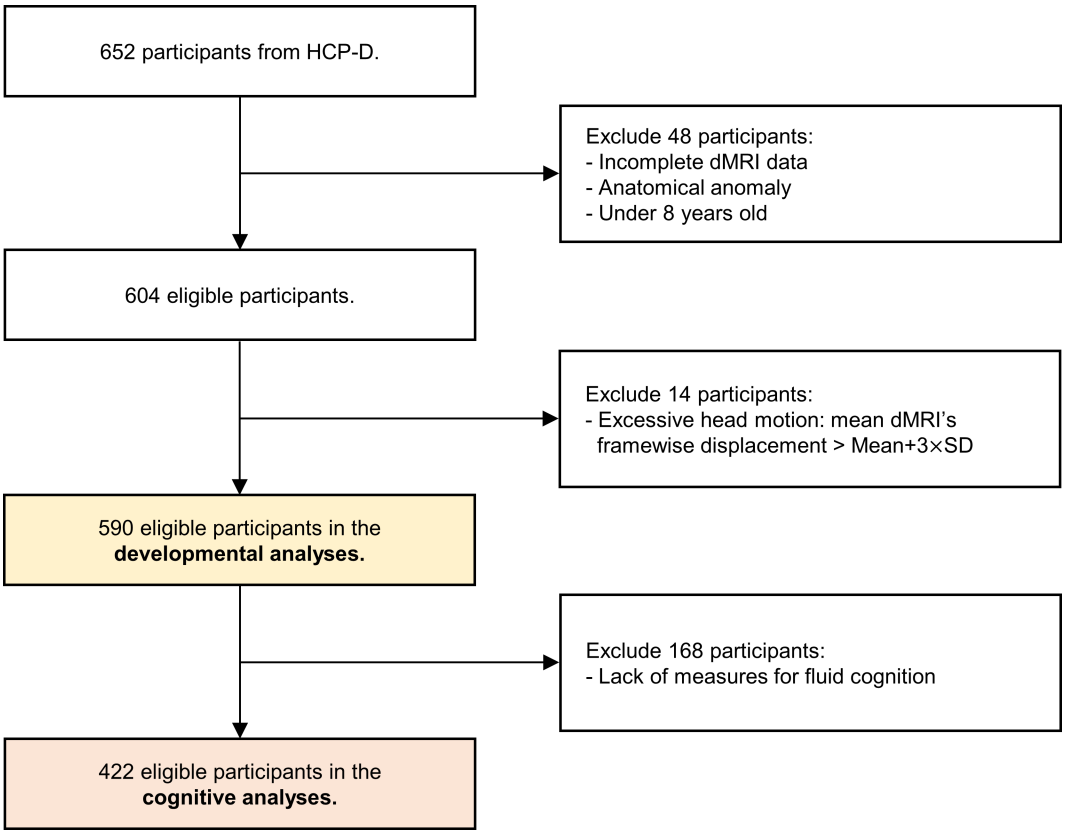

Figure S1. Flowchart of inclusion and exclusion for participants in the HCP-D dataset. HCP-D: the Lifespan Human Connectome Project Development; dMRI: diffusion magnetic resonance imaging; SD: standard deviation.

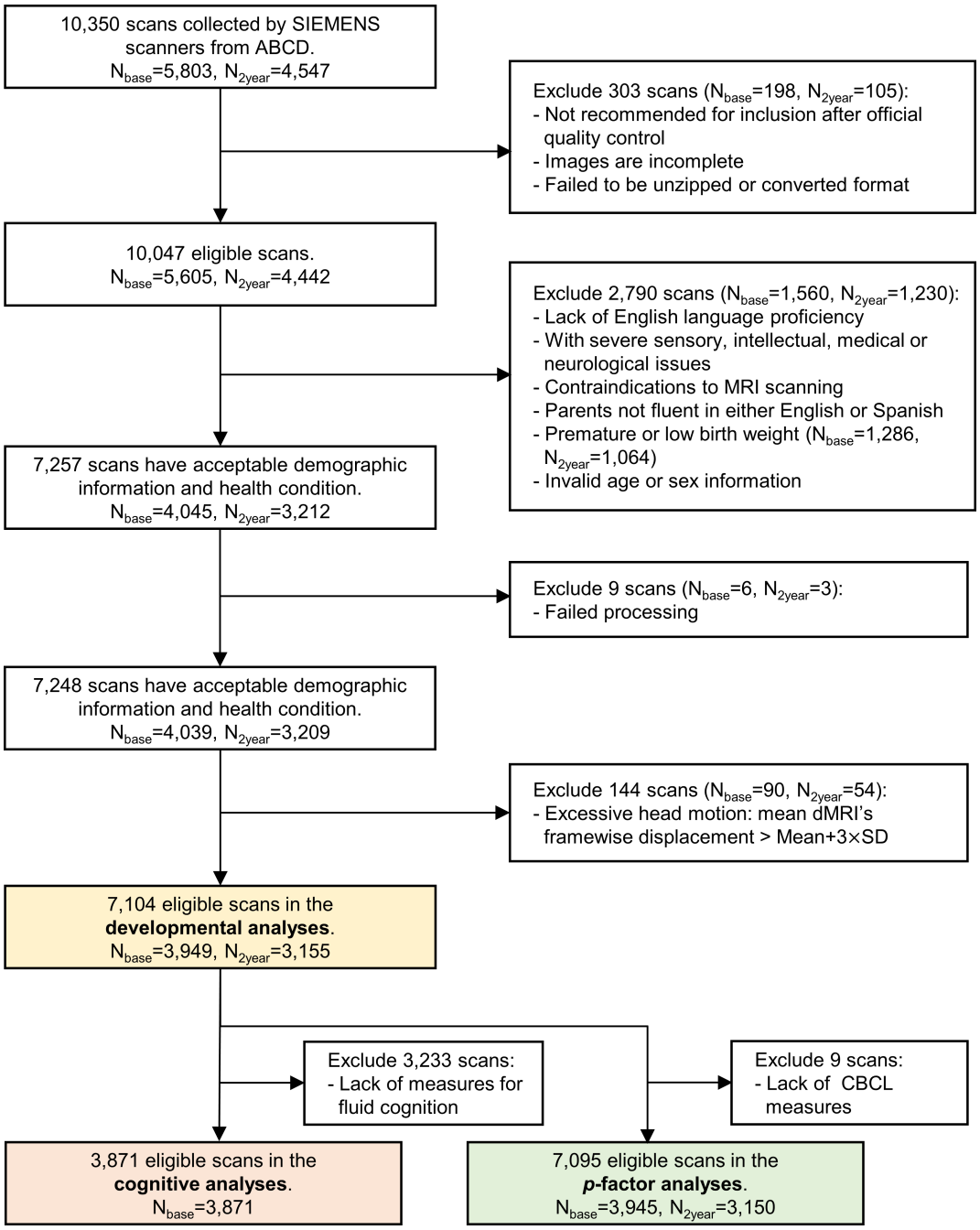

Figure S2. Flowchart of inclusion and exclusion for participants in the ABCD dataset. ABCD: the Adolescent Brain Cognitive Development; CBCL: Child Behavior Checklist.

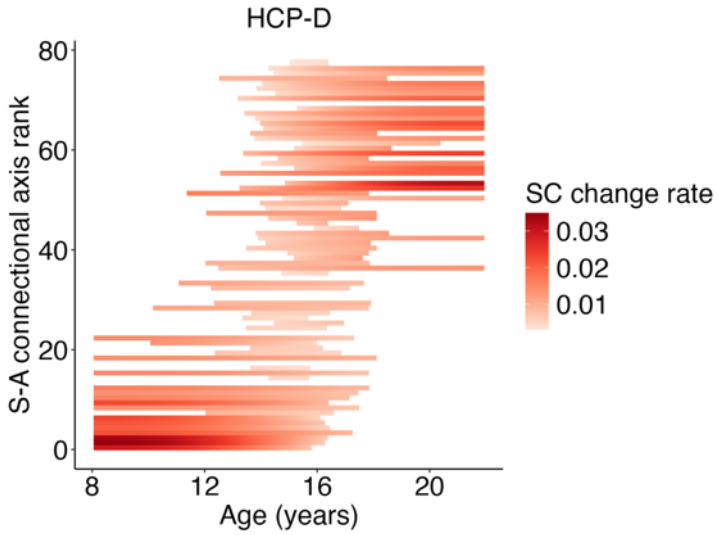

Figure S3. Significant developmental rates of the large-scale structural connections in the HCP-D dataset. The rate of developmental changes of the large-scale structural connections were measured using the first derivatives at 1,000 age points evenly sampled from the age range of 8.1 to 21.9 years. Each row represents an edge, with colors coded based on the magnitudes and direction of the significant developmental rates ($P_{FDR} < 0.05$). Insignificant developmental rates are shown in white. Since all significant derivatives are above zero, we used different shades of red to indicate their magnitudes. SC: structural connectivity; S-A: sensorimotor-association.

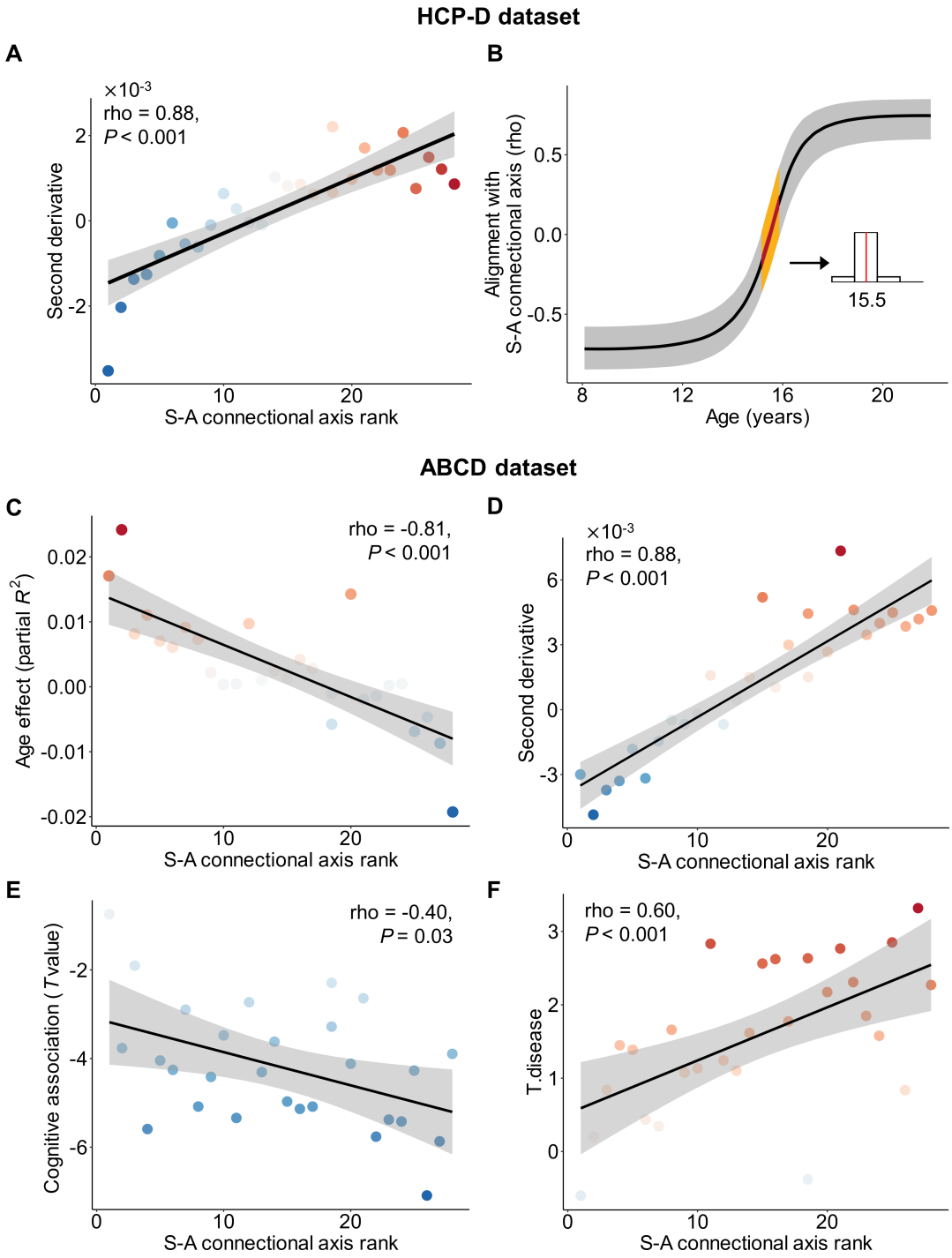

Figure S4. Sensitivity analyses with structural connectivity of the 7×7 connectome. **A**, In the HCP-D dataset, the second derivatives were highly correlated with the S-A connectional axis ranks across all structural connections (Spearman's rho = 0.88, $P <$ 0.001). **B**, The alignment between the spatial pattern of structural connectivity development and the S-A connectional axis evolves throughout youth. The black line represents the median correlation value, while the gray band indicates the 95% credible interval. The yellow ribbon denotes the age window of zero alignment. An inset histogram illustrates the distribution of ages with zero alignment with a median of 15.5 years. **C**, In the ABCD dataset, the age effects of structural connectivity strength

correlated with the S-A connectional axis ranks (Spearman's rho = -0.81, $P < 0.001$). **D**, The second derivatives of developmental changes also correlated with the S-A connectional axis ranks (Spearman's rho = 0.88, $P < 0.001$). **E**, The spatial pattern of cognitive association with structural connectivity strength was negatively correlated with the S-A connectional axis (Spearman's rho = -0.40, $P = 0.03$). **F**, The associations between structural connectivity strength and the general psychopathology factor (*p*-factor) were positively correlated with the S-A connectional axis ranks (Spearman's rho = 0.60, $P < 0.001$). HCP-D: the Lifespan Human Connectome Project Development; ABCD: the Adolescent Brain Cognitive Development; S-A: sensorimotor-association.

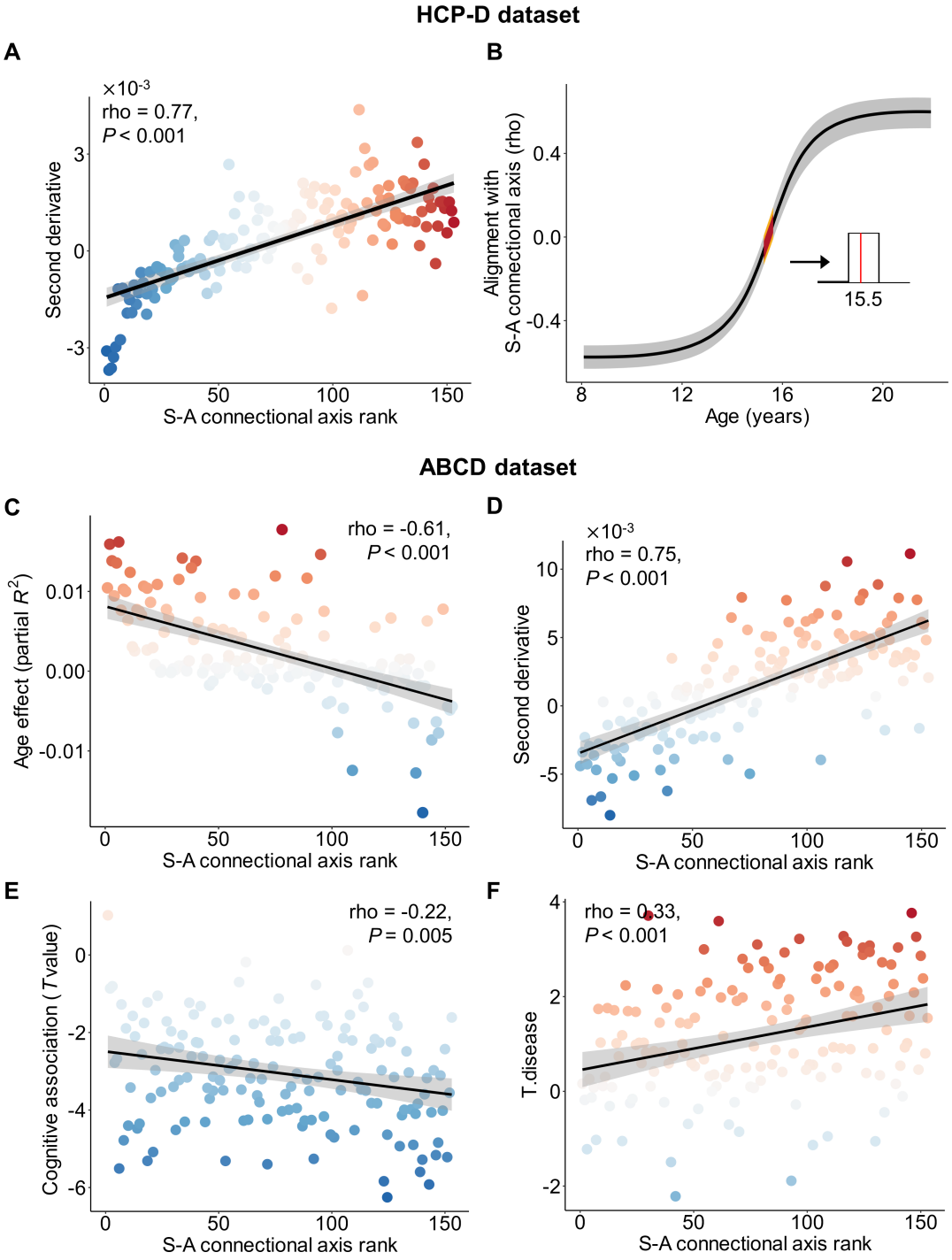

Figure S5. Sensitivity analyses with structural connectivity of the 17 × 17 connectome. A, In the HCP-D dataset, the second derivatives were highly correlated with the S-A connectional axis ranks across all structural connections (Spearman's rho = 0.77, $P < 0.001$). **B**, The alignment between the spatial pattern of structural connectivity development and the S-A connectional axis evolves throughout youth. The black line represents the median correlation value, while the gray band indicates the 95% credible interval. The yellow ribbon denotes the age window of zero alignment. An inset histogram illustrates the distribution of ages with zero alignment, with a median of 15.5 years. **C**, In the ABCD dataset, the age effects of structural connectivity strength

correlated with the S-A connectional axis ranks (Spearman's rho = -0.61, $P < 0.001$). **D**, The second derivatives of developmental changes also correlated with the S-A connectional axis ranks (Spearman's rho = 0.75, $P < 0.001$). **E**, The spatial pattern of cognitive association with structural connectivity strength was negatively correlated with the S-A connectional axis (Spearman's rho = -0.22, $P = 0.005$). **F**, The associations between structural connectivity strength and the general psychopathology factor (*p*-factor) were positively correlated with the S-A connectional axis ranks (Spearman's rho = 0.33, $P < 0.001$). S-A: sensorimotor-association. HCP-D: the Lifespan Human Connectome Project Development; ABCD: the Adolescent Brain Cognitive Development; S-A: sensorimotor-association.

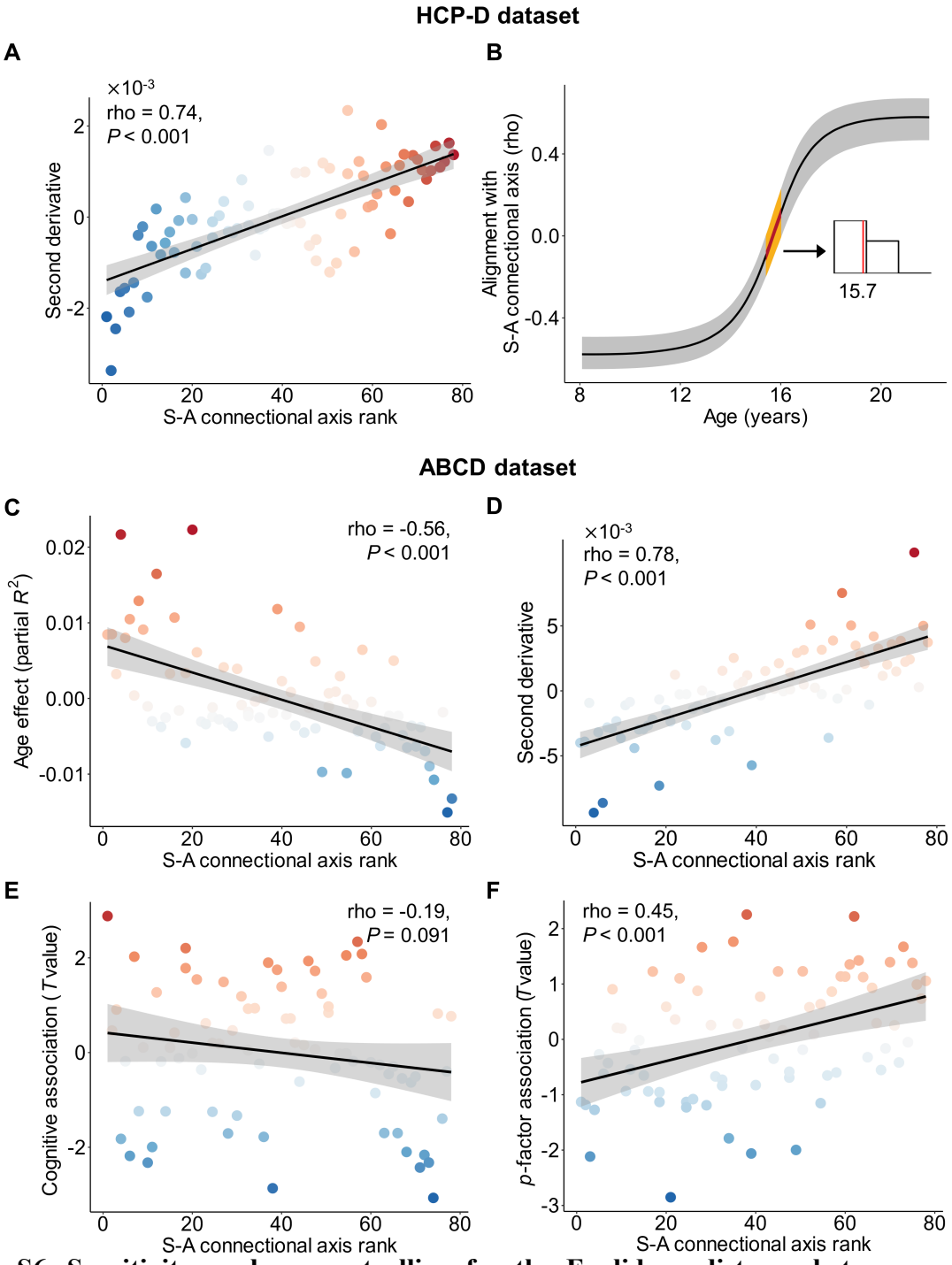

Figure S6. Sensitivity analyses controlling for the Euclidean distance between pairwise systems. A, In the HCP-D dataset, the second derivatives remained highly correlated with the S-A connectional axis ranks after controlling for the distribution of Euclidean distance between pairwise systems (Spearman's rho = 0.74, $P < 0.001$). **B**, The alignment between the spatial pattern of structural connectivity development and the S-A connectional axis evolves throughout youth, exhibiting a consistent pattern as in the primary result. The black line represents the median correlation value, while the gray band indicates the 95% credible interval. The yellow ribbon

denotes the age window of zero alignment. An inset histogram illustrates the distribution of ages with zero alignment, with a median of 15.7 years. **C**, In the ABCD dataset, the age effects of structural connectivity strength remained correlated with the S-A connectional axis ranks (Spearman's rho = -0.56, $P < 0.001$). **D**, The second derivatives of developmental changes also correlated with the S-A connectional axis ranks across all connections (Spearman's rho = 0.78, $P < 0.001$). **E**, The spatial pattern of cognitive association with structural connectivity strength showed a weak negative correlation with the S-A connectional axis (Spearman's rho = -0.19, $P = 0.091$). **F**, The associations between structural connectivity strength and the general psychopathology factor (*p*-factor) were positively correlated with the S-A connectional axis ranks (Spearman's rho = 0.45, $P < 0.001$). The y-axis in the figures above represents the residuals of the corresponding statistic matrices after regressing out the Euclidean distance of pairwise systems. HCP-D: the Lifespan Human Connectome Project Development; ABCD: the Adolescent Brain Cognitive Development; S-A: sensorimotor-association.

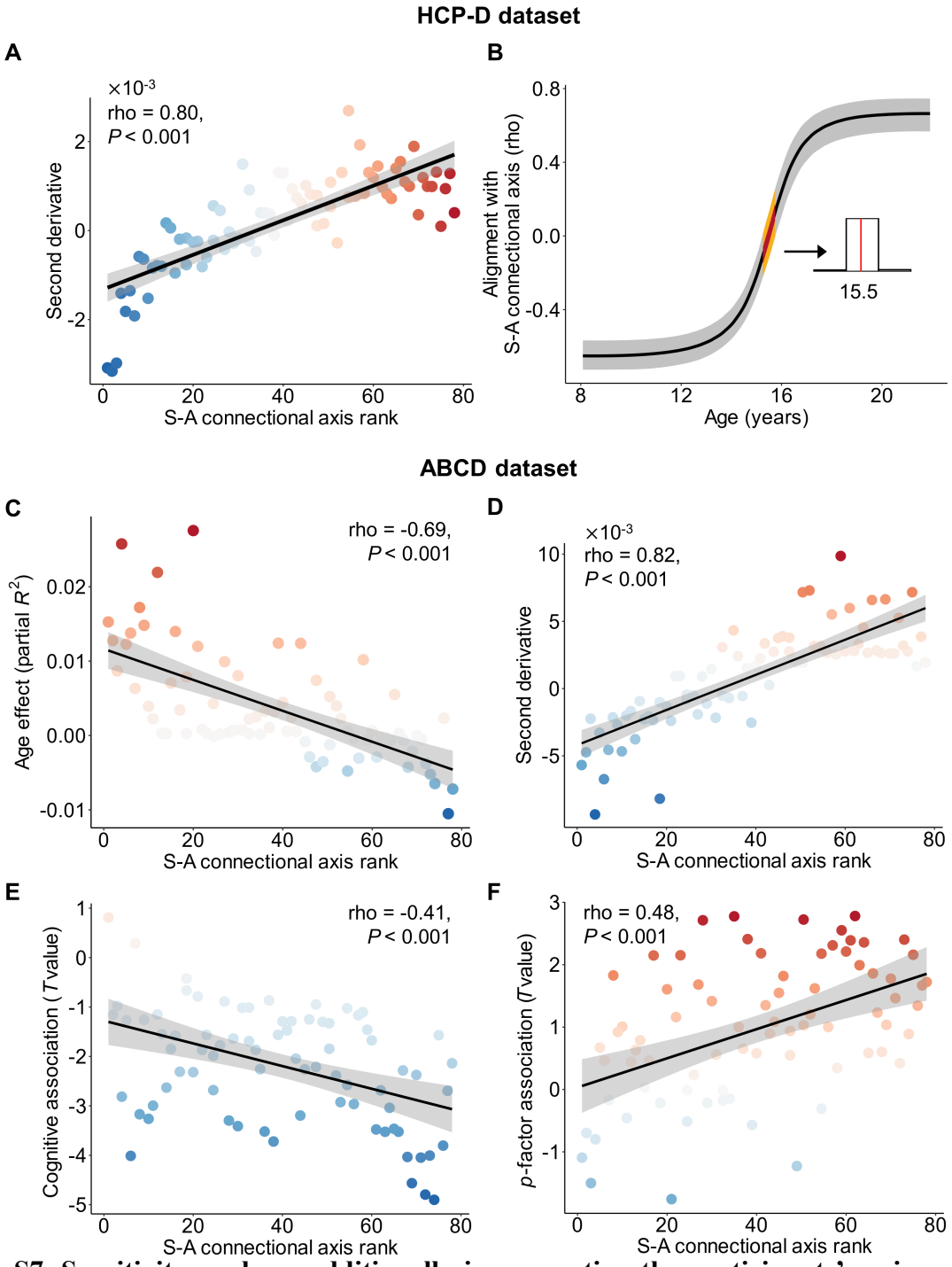

Figure S7. Sensitivity analyses additionally incorporating the participants' socioeconomic status as a covariate. A, In the HCP-D dataset, the second derivatives remained highly correlated with the S-A connectional axis ranks after additionally incorporating socioeconomic status as a covariate (Spearman's rho = 0.80, $P < 0.001$). **B**, The alignment between the spatial pattern of structural connectivity development and the S-A connectional axis evolves throughout youth, exhibiting a consistent pattern as in the primary result. The black line represents the median correlation value, while the gray band indicates the 95% credible interval. The yellow ribbon

denotes the age window of zero alignment. An inset histogram illustrates the distribution of ages with zero alignment, with a median of 15.5 years. **C**, In the ABCD dataset, the age effects of structural connectivity strength remained correlated with the S-A connectional axis ranks (Spearman's rho = -0.69, $P < 0.001$). **D**, The second derivatives of developmental changes also correlated with the S-A connectional axis ranks across all connections (Spearman's rho = 0.82, $P < 0.001$). **E**, The spatial pattern of cognitive association with structural connectivity strength showed a weak negative correlation with the S-A connectional axis (Spearman's rho = -0.41, $P < 0.001$). **F**, The associations between structural connectivity strength and the general psychopathology factor (*p*-factor) were positively correlated with the S-A connectional axis ranks (Spearman's rho = 0.48, $P < 0.001$). HCP-D: the Lifespan Human Connectome Project Development; ABCD: the Adolescent Brain Cognitive Development; S-A: sensorimotor-association.

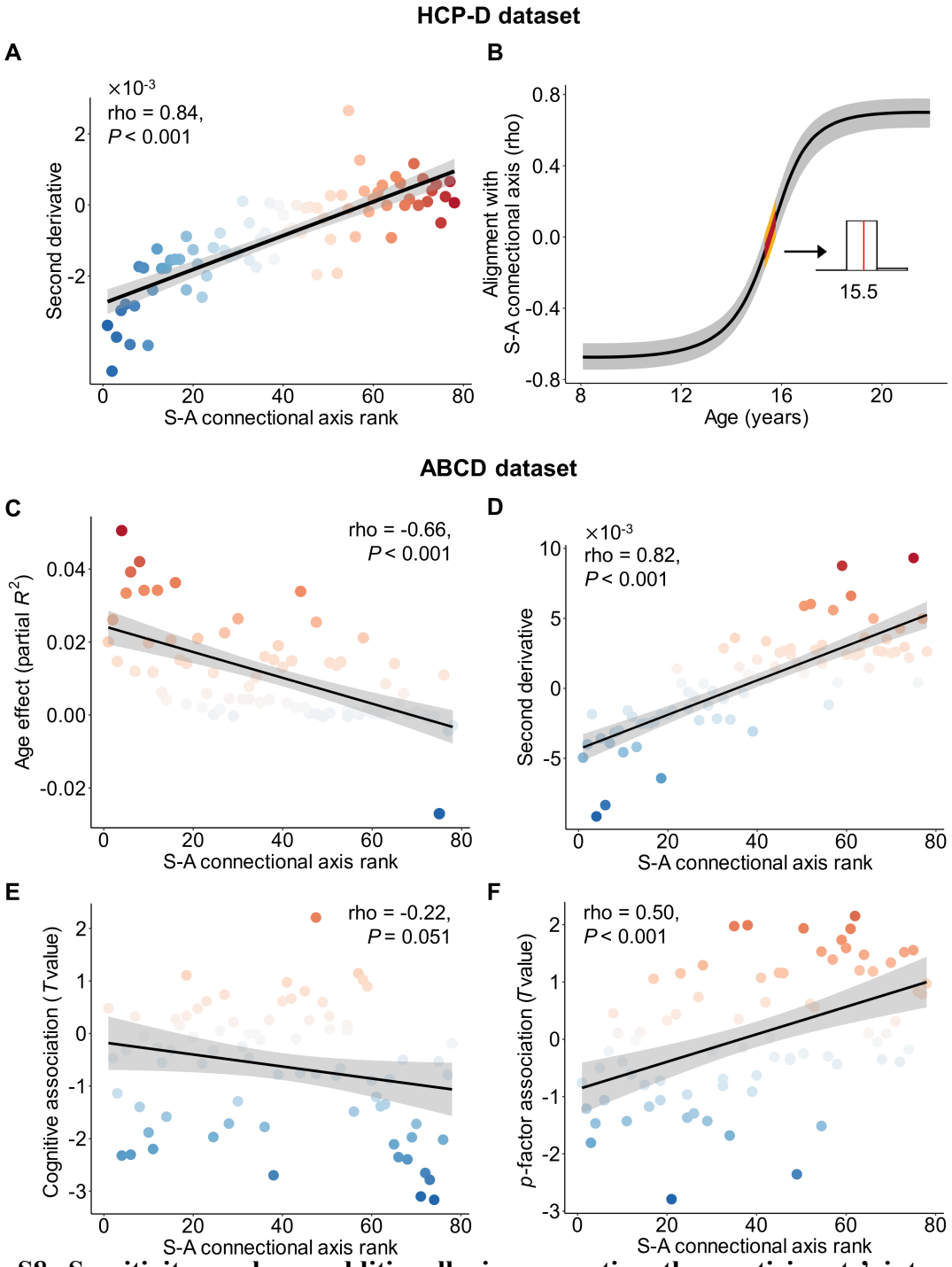

Figure S8. Sensitivity analyses additionally incorporating the participants' intracranial volume as a covariate. A, In the HCP-D dataset, the second derivatives remained highly correlated with the S-A connectional axis ranks after additionally incorporating intracranial as a covariate (Spearman's rho = 0.84, $P < 0.001$). **B**, The alignment between the spatial pattern of structural connectivity development and the S-A connectional axis evolves throughout youth, exhibiting a consistent pattern as in the primary result. The black line represents the median correlation value, while the gray band indicates the 95% credible interval. The yellow ribbon

denotes the age window of zero alignment. An inset histogram illustrates the distribution of ages with zero alignment, with a median of 15.5 years. **C**, In the ABCD dataset, the age effects of structural connectivity strength remained correlated with the S-A connectional axis ranks (Spearman's rho = -0.66, $P < 0.001$). **D**, The second derivatives of developmental changes also correlated with the S-A connectional axis ranks across all connections (Spearman's rho = 0.82, $P < 0.001$). **E**, The spatial pattern of cognitive association with structural connectivity strength showed a weak negative correlation with the S-A connectional axis (Spearman's rho = -0.22, $P = 0.051$). **F**, The associations between structural connectivity strength and the general psychopathology factor (*p*-factor) were positively correlated with the S-A connectional axis ranks (Spearman's rho = 0.50, $P < 0.001$). HCP-D: the Lifespan Human Connectome Project Development; ABCD: the Adolescent Brain Cognitive Development; S-A: sensorimotor-association.

Table S1. Demographic and cognitive characteristics of participants from the HCP-D dataset.

	HCP-D dataset
N	590
Age (years) (mean (SD))	14.72 (3.92)
Sex = Male (%)	273 (46.3)
Handedness (%)	
Right-handed	519 (88.0)
Left-handed	43 (7.3)
Mixed handed	28 (4.7)
Race/ethnicity (%)	
Hispanic	86 (14.6)
Non-Hispanic Asian	43 (7.5)
Non-Hispanic Black	56 (9.5)
Non-Hispanic White	344 (58.3)
Others	61 (10.3)
Fluid composite scores (mean (SD))	107.76 (12.75)
Mean FD (mean (SD))	0.66 (0.20)
Sites (%)	
Harvard	198 (33.6)
UMinn	156 (26.4)
UCLA	105 (17.8)
WashU	131 (22.2)
Intracranial volume (mm^3) (mean (SD))	1598201.51 (154010.77)
Family income-to-needs ratio	5.48 (6.04)

Note: The number of participants and percentages were displayed for categorical variables, while mean and standard deviation (SD) were provided for numeric variables. Ages in months and sex were extracted from 'HCD_LS_2.0_subject_completeness.csv' in the HCP-D dataset. Ages were converted to years by dividing by 12. Handedness scores derived from 'edinburgh_hand01.txt' were converted into a 3-level factor. Scores over 60 were defined as right-handed, under -60 as left-handed, and those in the middle as mixed-handed(Edlin et al., 2015). Race was obtained from 'socdem01.txt'. Fluid composite scores without age correction were derived from 'cogcomp01.txt'. Mean framewise displacement (FD) measures head motion during diffusion MRI scanning(Power et al., 2014). Site information was derived from 'ndar_subject01.txt'. The family income-to-needs ratio was calculated by dividing the annual family income ('socdem01.txt') by the federal poverty line for the year of the interview and the family size.

Table S2. Demographic, cognitive, and psychiatric characteristics of participants in the ABCD dataset.

	Baseline	Two-year follow-up
N	3949	3155
Age (years) (mean (SD))	9.93 (0.63)	11.95 (0.65)
Sex = male (%)	2075 (52.5)	1701 (53.9)
Race/ethnicity (%)		
Hispanic	678 (17.2)	525 (16.6)
Non-Hispanic Asian	68 (1.7)	41 (1.3)
Non-Hispanic Black	575 (14.6)	476 (15.1)
Non-Hispanic White	2257 (57.2)	1817 (57.6)
Other	371 (9.4)	296 (9.4)
Handedness (%)		
Right-handed	3166(80.2)	2510(79.6)
Left-handed	270(6.8)	230(7.3)
Mixed handed	513(13.0)	415(13.2)
Fluid composite scores (mean (SD))	92.53 (10.12)	-
P-factor (mean (SD))	0.07(0.83)	0.04(0.82)
Mean FD (mean (SD))	0.55 (0.21)	0.53 (0.20)
Sites (%)		
Site02	174(4.4)	161(5.1)
Site03	308(7.8)	248(7.9)
Site05	225(5.7)	183(5.8)
Site06	392(9.9)	314(10.0)
Site07	153(3.9)	123(3.9)
Site09	258(6.5)	162(5.1)
Site11	268(6.8)	190(6.0)
Site12	444(11.2)	317(10.0)
Site14	241(6.1)	176(5.6)
Site15	204(5.2)	168(5.3)
Site16	696(17.6)	581(18.4)
Site20	219(5.5)	226(7.2)
Site21	367(9.3)	306(9.7)
Intracranial volume (mm^3) (mean (SD))	1534157.62(132994.37)	1561853.71(140683.69)
Family income-to-needs ratio	3.80(2.35)	3.81(2.29)

Note: The number of participants and percentages were displayed for categorical variables, while mean and standard deviation (SD) were displayed for numeric variables. Ages in months and site information were obtained from 'abcd_y_lt.csv'. Ages were then converted to years by dividing by 12. Sex and race/ethnicity were extracted from 'abcd_p_demo.csv'. Three-factor handedness

was acquired from ‘nc_y_ehis.csv’. Fluid composite scores without age correction were obtained from ‘nc_y_nihtb. csv’. General psychopathology factor (*p*-factor) scores were derived from the Child Behavior Checklist (CBCL). The family income-to-needs ratio was calculated by dividing the annual family income (‘abcd_p_demo. csv’) by the federal poverty line for the year of the interview and the family size.

References

Edlin, J.M., Leppanen, M.L., Fain, R.J., Hacklander, R.P., Hanaver-Torrez, S.D., and Lyle, K.B. (2015). On the use (and misuse?) of the Edinburgh Handedness Inventory. Brain Cogn *94*, 44-51. 10.1016/j.bandc.2015.01.003.

Power, J.D., Mitra, A., Laumann, T.O., Snyder, A.Z., Schlaggar, B.L., and Petersen, S.E. (2014). Methods to detect, characterize, and remove motion artifact in resting state fMRI. NeuroImage *84*, 320-341. https://doi.org/10.1016/j.neuroimage.2013.08.048.